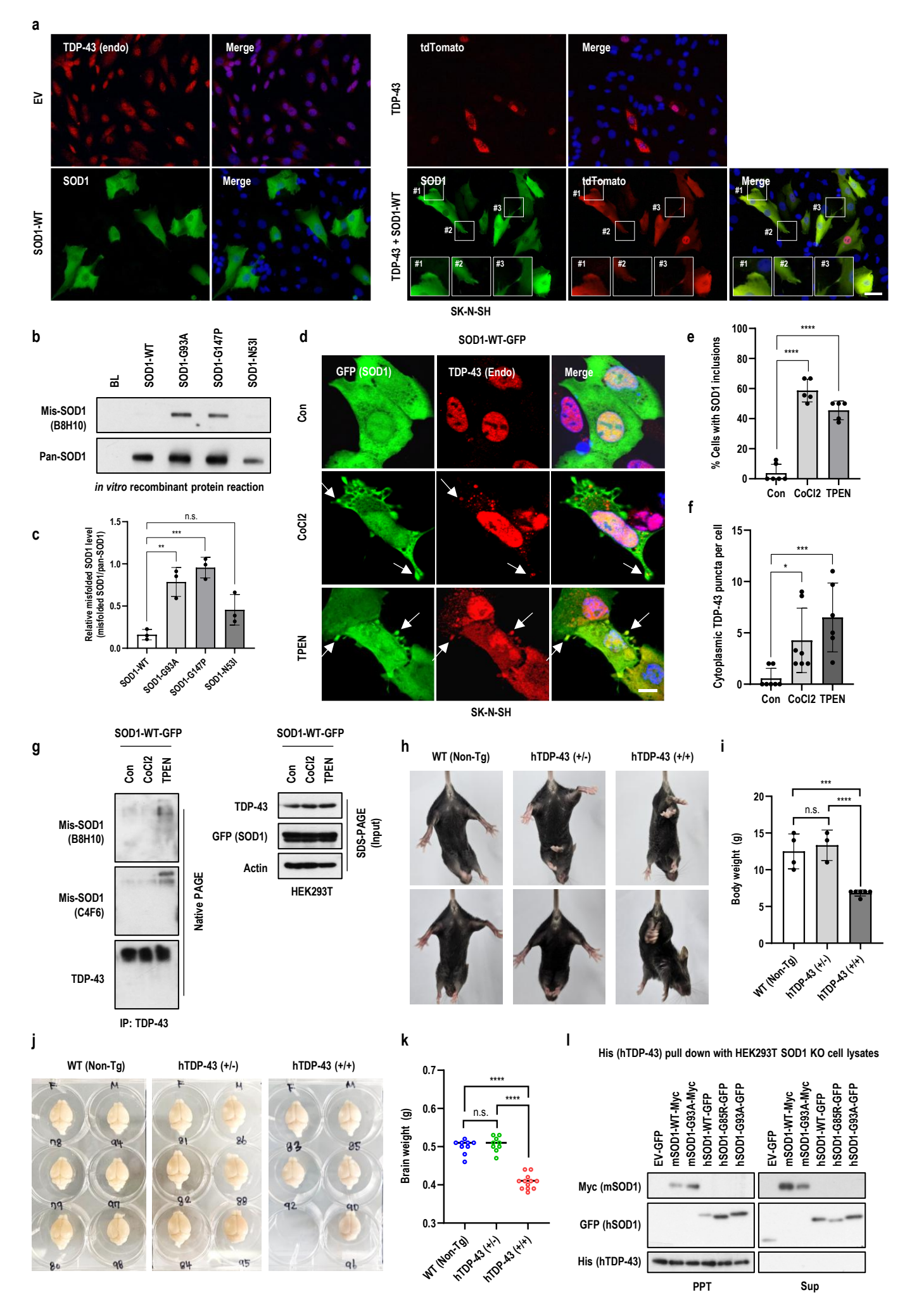

a
EV
SOD1-WT
TDP-43 (endo)
Merge
SOD1
Merge
TDP-43
tdTomato
Merge
TDP-43 + SOD1-WT
SOD1
tdTomato
Merge
#1
#2
#3
SK-N-SH
b
BL
SOD1-WT
SOD1-G93A
SOD1-G147P
SOD1-N53I
Mis-SOD1 (B8H10)
Pan-SOD1
in vitro recombinant protein reaction
c
Relative misfolded SOD1 level (misfolded SOD1/pan-SOD1)
n.s.
***
**
SOD1-WT
SOD1-G93A
SOD1-G147P
SOD1-N53I
d
SOD1-WT-GFP
GFP (SOD1)
TDP-43 (Endo)
Merge
Con
CoCl2
TPEN
SK-N-SH
e
% Cells with SOD1 inclusions
****
****
Con
CoCl2
TPEN
f
Cytoplasmic TDP-43 puncta per cell
***
*
Con
CoCl2
TPEN
g
SOD1-WT-GFP
Con
CoCl2
TPEN
Mis-SOD1 (B8H10)
Mis-SOD1 (C4F6)
TDP-43
Native PAGE
IP: TDP-43
SOD1-WT-GFP
TDP-43
GFP (SOD1)
Actin
SDS-PAGE (Input)
HEK293T
h
WT (Non-Tg)
hTDP-43 (+/-)
hTDP-43 (+/+)
i
Body weight (g)
***
****
n.s.
WT (Non-Tg)
hTDP-43 (+/-)
hTDP-43 (+/+)
j
WT (Non-Tg)
hTDP-43 (+/-)
hTDP-43 (+/+)
k
Brain weight (g)
****
****
n.s.
WT (Non-Tg)
hTDP-43 (+/-)
hTDP-43 (+/+)
l
His (hTDP-43) pull down with HEK293T SOD1 KO cell lysates
EV-GFP
mSOD1-WT-Myc
mSOD1-G93A-Myc
hSOD1-WT-GFP
hSOD1-G85R-GFP
hSOD1-G93A-GFP
Myc (mSOD1)
GFP (hSOD1)
His (hTDP-43)
PPT
Sup

Fig. S1 The robust sALS pathology of hTDP-43 Tg mice. a Wider-field images showing increased formation of WT-SOD1 inclusions upon TDP-43 overexpression in SK-N-SH cells. Scale bar, 50 μm. **b, c** The misfolded SOD1 antibody (B8H10; labeled as Mis-SOD1) preferentially detected mutant SOD1 (G93A) and the trimer-stabilizing mutant (G147P) compared with WT-SOD1 and the trimer-destabilizing mutant (N53I). Representative dot blot images (**b**) and quantification (**c**) are presented. **d-f** Upon exposure to cellular stress, SOD1 inclusions colocalized with cytoplasmic TDP-43 puncta (**d**). SOD1 inclusion-positive cells (**e**) and cytoplasmic TDP-43 puncta per cell (**f**) were counted, and the percentages are presented as mean ± SD. Scale bar, 10 μm. *$p < 0.05$, ***$p < 0.001$, ****$p < 0.0001$. **g** Cellular stress induced B8H10- and C4F6-reactive SOD1 oligomeric species that were interacted with TDP-43. **h** hTDP-43 (+/+) mice exhibited an abnormal hindlimb phenotype compared with WT (Non-Tg). **i** hTDP-43 (+/+) mice showed significantly reduced body weights compared with WT (Non-Tg). ***$p < 0.001$, ****$p < 0.0001$. **j, k** hTDP-43 (+/+) mice showed significantly reduced brain size (**j**) and weights (**k**). *** $p < 0.001$, ****$p < 0.0001$. **l** Both hSOD1 and mSOD1 interacted with hTDP-43, although mSOD1 showed weaker binding than hSOD1. HEK293T SOD1-KO cell lysates expressing mSOD1 or hSOD1 were incubated with His-TDP-43 proteins.

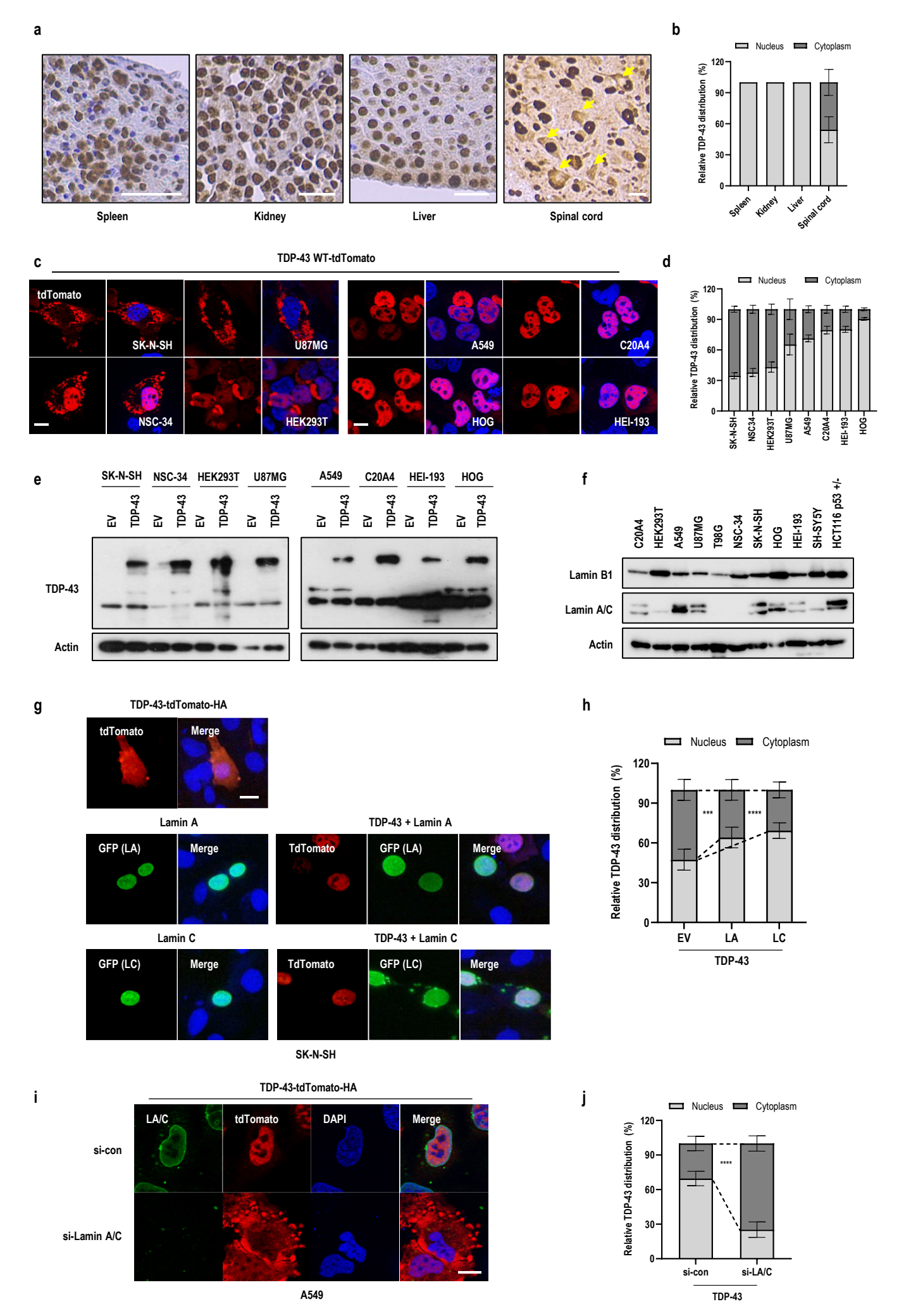

a
Spleen
Kidney
Liver
Spinal cord
b
Nucleus
Cytoplasm
Relative TDP-43 distribution (%)
120
90
60
30
0
Spleen
Kidney
Liver
Spinal cord
c
TDP-43 WT-tdTomato
tdTomato
SK-N-SH
U87MG
A549
C20A4
NSC-34
HEK293T
HOG
HEI-193
d
Nucleus
Cytoplasm
Relative TDP-43 distribution (%)
SK-N-SH
NSC34
HEK293T
U87MG
A549
C20A4
HEI-193
HOG
e
SK-N-SH
NSC-34
HEK293T
U87MG
A549
C20A4
HEI-193
HOG
EV
TDP-43
TDP-43
Actin
f
C20A4
HEK293T
A549
U87MG
T98G
NSC-34
SK-N-SH
HOG
HEI-193
SH-SY5Y
HCT116 p53 +/-
Lamin B1
Lamin A/C
Actin
g
TDP-43-tdTomato-HA
tdTomato
Merge
Lamin A
GFP (LA)
Merge
TDP-43 + Lamin A
TdTomato
GFP (LA)
Merge
Lamin C
GFP (LC)
Merge
TDP-43 + Lamin C
TdTomato
GFP (LC)
Merge
SK-N-SH
h
Nucleus
Cytoplasm
Relative TDP-43 distribution (%)
120
90
60
30
0
***
****
EV
LA
LC
TDP-43
i
TDP-43-tdTomato-HA
LA/C
tdTomato
DAPI
Merge
si-con
si-Lamin A/C
A549
j
Nucleus
Cytoplasm
Relative TDP-43 distribution (%)
120
90
60
30
0
****
si-con
si-LA/C
TDP-43

Fig. S2 TDP-43 overexpression induces cytoplasmic TDP-43 mislocalization. a, b Cytoplasmic TDP-43 mislocalization was observed in a neuron-specific manner in hTDP-43 (+/+) mice. The relative nuclear and cytoplasmic distribution of TDP-43 was quantified by cell counting, and the percentages are presented as mean ± SD (**b**). Spleen (n=4), kidney (n=4), liver (n=4), spinal cord (n=4). Scale bars, 20 μm**. c, d** Cytoplasmic TDP-43 mislocalization occurred in a neuronal cell line-dependent manner (**c**). Scale bar, 10 μm**.** The relative nuclear and cytoplasmic distribution of TDP-43 was quantified by cell counting, and the percentages are presented as mean ± SD (**d**). SK-N-SH (n=5), NSC-34 (n=5), HEK293T (n=7), U87MG (n=4), A549 (n=5), C20A4 (n=7), HEI-193 (n=5), HOG (n=5). **e** TDP-43 overexpression levels were comparable across the different cell lines. **f** TDP-43 mislocalization exhibited a dependency on Lamin A/C expression, which constitutes a key component of the nuclear envelope. **g, h** Overexpression of Lamin A or Lamin C reduced cytoplasmic TDP-43 mislocalization in SK-N-SH cells (**g**). Scale bar, 10 μm. The relative nuclear and cytoplasmic distribution of TDP-43 was quantified by cell counting, and the percentages are presented as mean ± SD (**h**). EV (n=8), LA (n=8), LC (n=8). ***$p < 0.001$, ****$p < 0.0001$. **i, j** Lamin A/C knockdown induced cytoplasmic TDP-43 mislocalization in A549 cells (**i**). Scale bar, 20 μm. The relative nuclear and cytoplasmic distribution of TDP-43 was quantified by cell counting, and the percentages are presented as mean ± SD (**j**). si-con (n=6), si-LA/C (n=7). ****$p < 0.0001$.

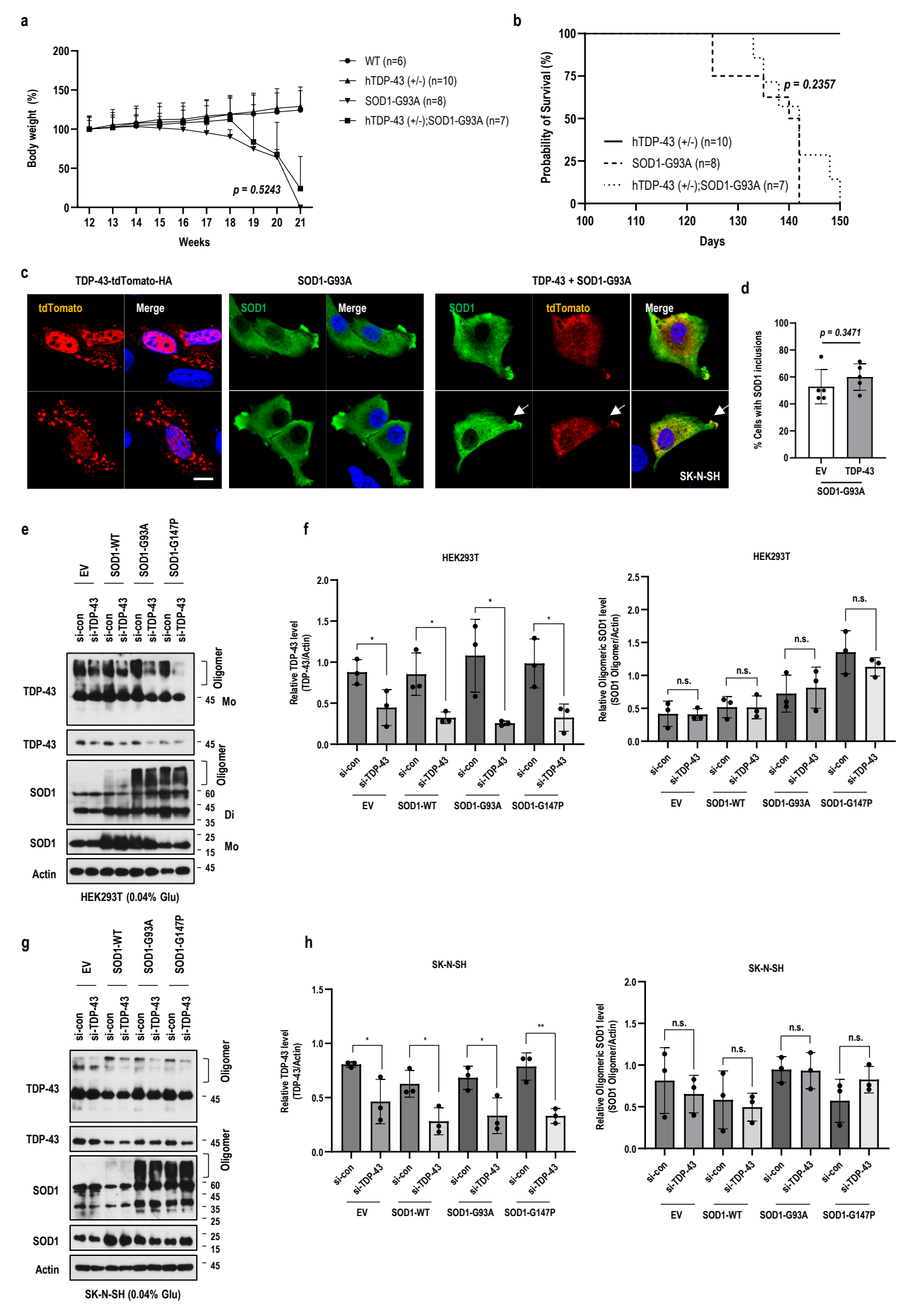

a
Body weight (%)
Weeks
WT (n=6)
hTDP-43 (+/-) (n=10)
SOD1-G93A (n=8)
hTDP-43 (+/-);SOD1-G93A (n=7)
p = 0.5243
b
Probability of Survival (%)
Days
p = 0.2357
hTDP-43 (+/-) (n=10)
SOD1-G93A (n=8)
hTDP-43 (+/-);SOD1-G93A (n=7)
c
TDP-43-tdTomato-HA
SOD1-G93A
TDP-43 + SOD1-G93A
tdTomato
Merge
SOD1
SK-N-SH
d
% Cells with SOD1 inclusions
p = 0.3471
EV
TDP-43
SOD1-G93A
e
EV
SOD1-WT
SOD1-G93A
SOD1-G147P
si-con
si-TDP-43
TDP-43
Oligomer
Mo
Di
SOD1
Actin
HEK293T (0.04% Glu)
f
HEK293T
Relative TDP-43 level (TDP-43/Actin)
Relative Oligomeric SOD1 level (SOD1 Oligomer/Actin)
n.s.
g
SK-N-SH (0.04% Glu)
h
SK-N-SH

Fig. S3 TDP-43 did not accelerate the pathology of SOD1-G93A Tg mice. a No significant changes in body weight were observed between hSOD1-G93A and hTDP-43 (+/-);hSOD1-G93A mice. **b** Kaplan Meier survival analysis indicated that hTDP-43 (+/-);SOD1-G93A mice did not accelerate the disease progression of SOD1-G93A mice. **c, d** TDP-43 did not increase the number of MT-SOD1 inclusions (**c**). Scale bar, 10 μm. SOD1 inclusion-positive cells (white arrows) were counted and the percentages are shown as mean ± SD (**d**). **e-h** SOD1 oligomerization induced by SOD1-G93A or SOD1-G147P was unaffected by TDP-43 knockdown in HEK293T cells (**e**) and SK-N-SH cells (**g**). Quantification of TDP-43 or oligomeric SOD1 levels (**f, h**). *$p < 0.05$, **$p < 0.01$.

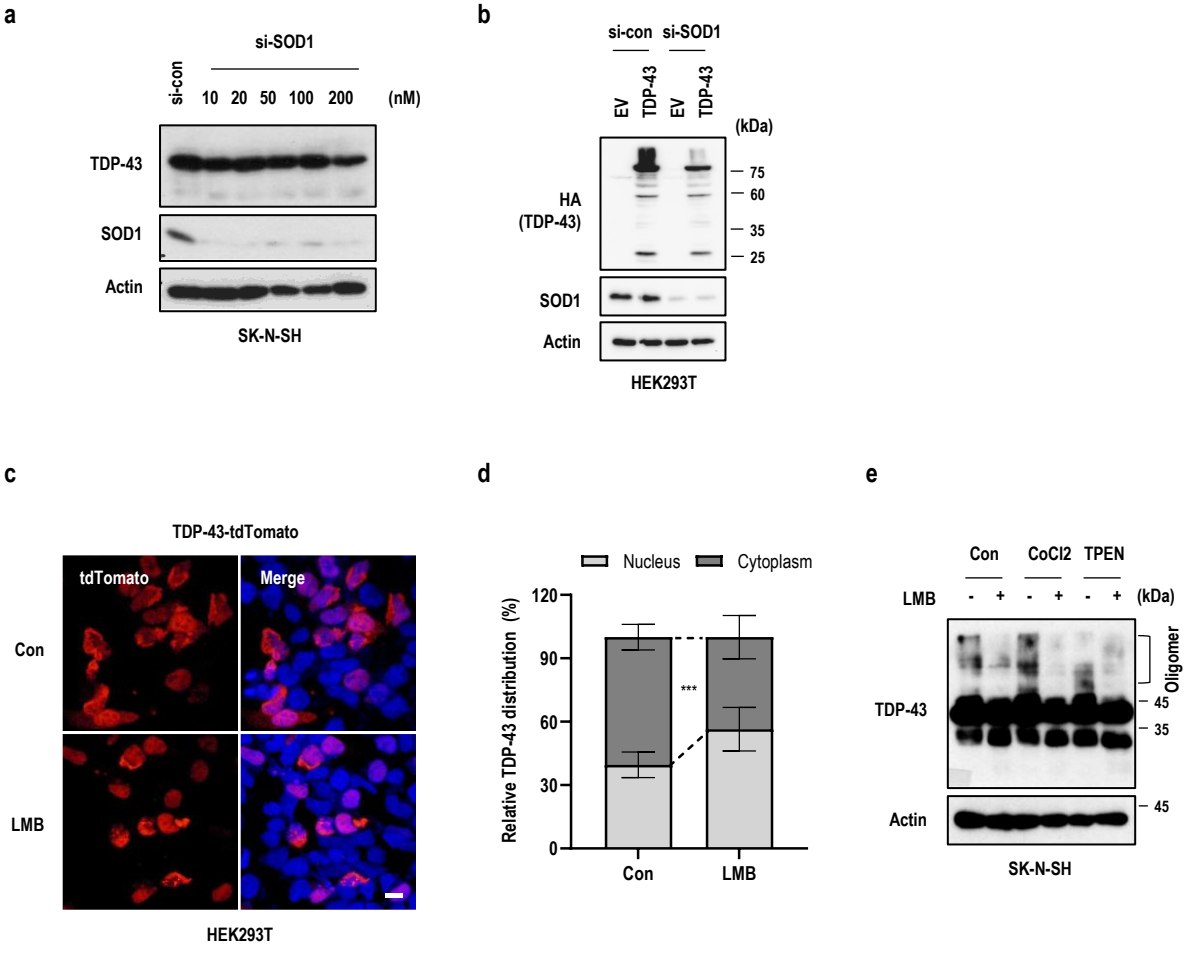
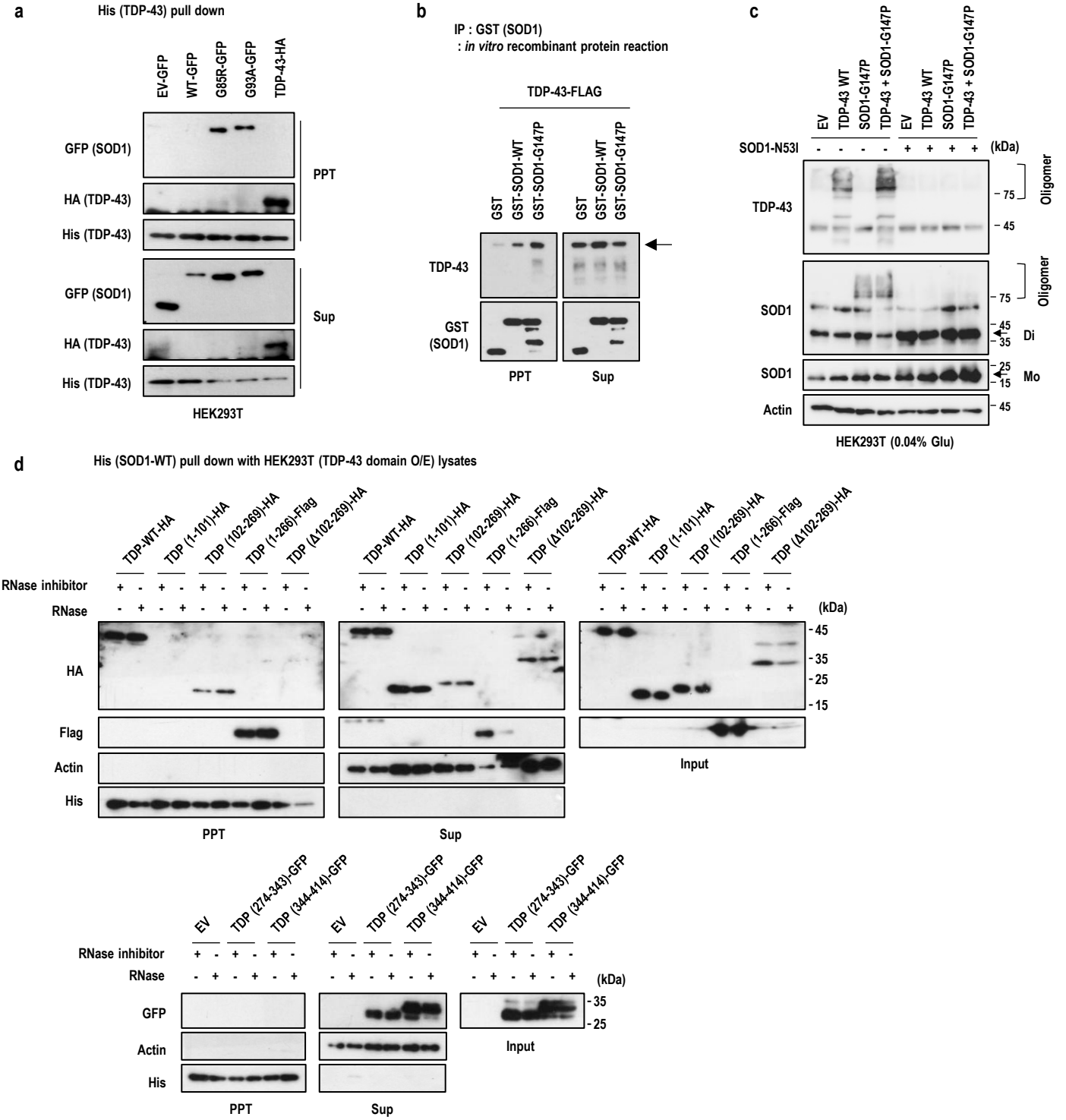

a
si-SOD1
si-con
10 20 50 100 200 (nM)
TDP-43
SOD1
Actin
SK-N-SH
b
si-con si-SOD1
EV TDP-43 EV TDP-43
(kDa)
HA
(TDP-43)
75
60
35
25
SOD1
Actin
HEK293T
c
TDP-43-tdTomato
tdTomato
Merge
Con
LMB
HEK293T
d
Nucleus Cytoplasm
Relative TDP-43 distribution (%)
120
90
60
30
0
***
Con
LMB
e
Con CoCl2 TPEN
LMB - + - + - + (kDa)
TDP-43
Oligomer
45
35
Actin
45
SK-N-SH

Fig. S4. SOD1 deficiency attenuates cytoplasmic TDP-43 mislocalization. a SOD1 knockdown efficiency was evaluated across different siRNA concentrations in SK-N-SH cells. **b** TDP-43 oligomerization induced by TDP-43 overexpression was reduced by SOD1 knockdown in HEK293T cells. **c, d** LMB (10 μM) treatment for 6 hr attenuated cytoplasmic TDP-43 mislocalization by TDP-43 overexpression (c). Scale bar, 10 μm. The relative nuclear and cytoplasmic distribution of TDP-43 was quantified by cell counting, and the percentages are presented as mean ± SD (d). Con (n=10), LMB (n=10). ***$p < 0.001$. **e** LMB attenuated cellular stress-induced TDP-43 oligomerization.



e

Predicted molecular interaction residues of TDP-43 RRM1–2 and the SOD1 trimer

SOD1 chain	PDB residue	SOD1 residue (canonical numbering)	TDP-43 residue	Interaction	Distance (Å)
A	Lys122	Lys122	Ser183	H-bond	1.7
A	Lys128	Lys128	Asn179	H-bond	1.671
A	Gly147	Gly147	Glu261	H-bond	2.046
A	Gly129	Gly129	Ser180	H-bond	2.259
A	Ser134	Ser134	Arg197	H-bond	1.798
A	Thr137	Thr137	Arg227	H-bond	2.445
A	Ser59	Ser59	Arg227	H-bond	1.811
A	Arg143	Arg143	Asn259	H-bond	2.148
A	Ser142	Ser142	Asn259	H-bond	2.277
A	Asp109	Asp109	Ser266	H-bond	1.856
A	Cys146	Cys146	Gln269	H-bond	2.314
A	Arg143	Arg143	Asp185	Salt bridge	2.685
A	Asp11	Asp11	Lys102	Salt bridge	2.682–2.941
A	Glu133	Glu133	Lys145	Salt bridge	2.540–2.636
A	Asp52	Asp52	Arg227	Salt bridge	3.022–3.214
A	Asp109	Asp109	Arg268	Salt bridge	3.644
B	Thr207	Thr54	Lys263	H-bond	1.662
B	Asp277	Asp124	Lys140	Salt bridge	2.667–2.724
B	Glu202	Glu49	Lys263	Salt bridge	2.495–2.755
C	Glu355	Glu49	Asn265	H-bond	2.245
C	Glu355	Glu49	His264	Salt bridge	2.888

f

Predicted binding affinity of SOD1 and TDP-43

No.	TDP-43	SOD1	Predicted binding affinity (kcal.mol^{-1})
1	RRM1-2	Trimer	-17.6
2	RRM1-2	Dimer	-11.4
3	RRM1-2	Monomer	-11.8
4	NTD	Trimer	-8.6
5	NTD	Dimer	-14.5
6	NTD	Monomer	-9.7

Fig. S5. SOD1 interacts with RRM motif of TDP-43. a TDP-43 exhibited stronger interaction with MT-SOD1 (G85R and G93A) than WT-SOD1. A pull-down assay was performed using recombinant His-TDP-43 and lysates from SOD1 expressing cells. **b** TDP-43 showed stronger interaction with SOD1 trimer-stabilizing mutant (G147P) than WT-SOD1. An immunoprecipitation (IP) assay was performed using recombinant TDP-43 and SOD1 proteins. **c** Oligomerization of SOD1 or TDP-43 induced by TDP-43 and/or SOD1-G147P overexpression was reduced by the SOD1 trimer-destabilizing mutant (N53I). **d** WT-SOD1 interacted with TDP-43 102-269 domain regardless of RNase treatment. **e** A table listing the predicted interacting residues at the docking interface is presented **f** The TDP-43 RRM1–2 domain (PDB ID 4BS2) showed a higher predicted binding affinity for trimeric SOD1 than for monomeric or dimeric SOD1 (PDB ID 1HL5). The TDP-43 NTD (N terminal domain, PDB ID 2N4P) was used as a negative control.

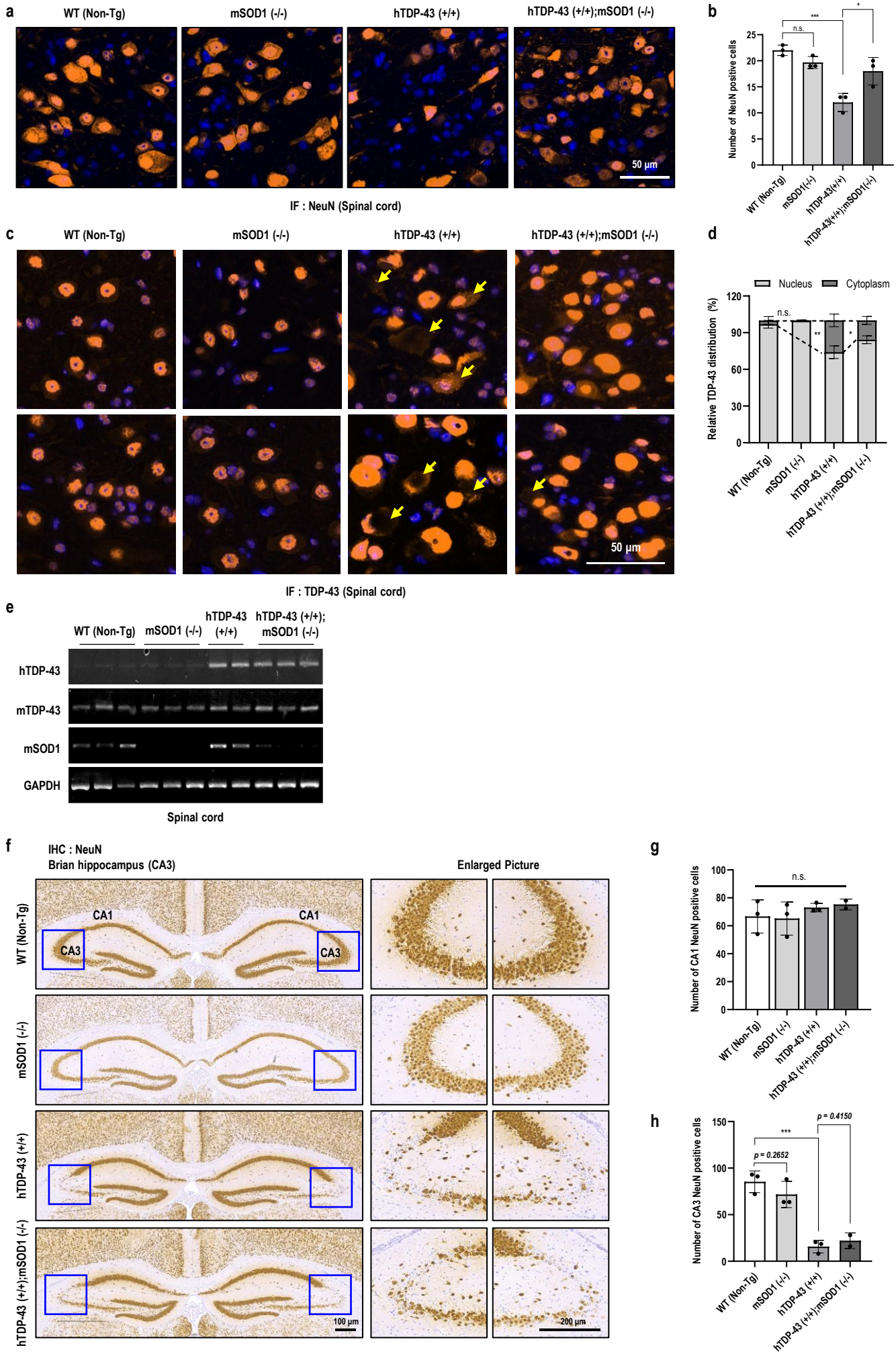

a
WT (Non-Tg)
mSOD1 (-/-)
hTDP-43 (+/+)
hTDP-43 (+/+);mSOD1 (-/-)
50 μm
IF : NeuN (Spinal cord)
b
Number of NeuN positive cells
n.s.
***
*
WT (Non-Tg)
mSOD1(-/-)
hTDP-43(+/+)
hTDP-43(+/+);mSOD1(-/-)
c
WT (Non-Tg)
mSOD1 (-/-)
hTDP-43 (+/+)
hTDP-43 (+/+);mSOD1 (-/-)
50 μm
IF : TDP-43 (Spinal cord)
d
Nucleus
Cytoplasm
Relative TDP-43 distribution (%)
n.s.
**
*
WT (Non-Tg)
mSOD1 (-/-)
hTDP-43 (+/+)
hTDP-43 (+/+);mSOD1 (-/-)
e
WT (Non-Tg)
mSOD1 (-/-)
hTDP-43 (+/+)
hTDP-43 (+/+); mSOD1 (-/-)
hTDP-43
mTDP-43
mSOD1
GAPDH
Spinal cord
f
IHC : NeuN
Brian hippocampus (CA3)
Enlarged Picture
WT (Non-Tg)
mSOD1 (-/-)
hTDP-43 (+/+)
hTDP-43 (+/+);mSOD1 (-/-)
CA1
CA3
100 μm
200 μm
g
Number of CA1 NeuN positive cells
n.s.
WT (Non-Tg)
mSOD1 (-/-)
hTDP-43 (+/+)
hTDP-43 (+/+);mSOD1 (-/-)
h
Number of CA3 NeuN positive cells
p = 0.2652
***
p = 0.4150
WT (Non-Tg)
mSOD1 (-/-)
hTDP-43 (+/+)
hTDP-43 (+/+);mSOD1 (-/-)

Fig. S6. SOD1 knockout ameliorates spinal cord, but not brain, pathology in hTDP-43 mice. a, b Reduced NeuN levels in hTDP-43 (+/+) mice were restored in hTDP-43 (+/+);mSOD1 (-/-) mice. Representative confocal immunofluorescence images of NeuN in cervical spinal cord sections from mice (**a**). Scale bar, 50 μm. The number of NeuN-positive cells was counted (**b**). *$p < 0.05$, ***$p < 0.001$. **c, d** Compared with WT mice (n=3), hTDP-43 (+/+) mice (n=3) exhibited increased cytoplasmic TDP-43 mislocalization (yellow arrows), which was reduced in hTDP-43 (+/+);mSOD1 (-/-) mice (n=3). mSOD1 (-/-) mice (n=3). Representative confocal immunofluorescence images of TDP-43 in cervical spinal cord sections from mice (**c**). Scale bar, 50 μm. The relative nuclear and cytoplasmic distribution of TDP-43 was quantified by cell counting, and the percentages are presented as mean ± SD (**d**). *$p < 0.05$, **$p < 0.01$. **e** Total TDP-43 expression was unchanged by mSOD1 knockout. RT-PCR analysis showed no changes in hTDP-43 or mTDP-43 mRNA levels **f-h** Neuronal loss in the hippocampal CA3 region observed in hTDP-43 (+/+) mice was not recovered by SOD1 deficiency (**f**). NeuN immunostaining of the brain hippocampus. Enlarged images of the CA3 region. Scale bar, 100 μm, enlarged images, 200 μm. No significant difference in the number of NeuN-positive cells was observed in the CA1 region (**g**). NeuN-positive cell numbers were reduced in the CA3 region of hTDP-43 (+/+) mice compared with WT mice and were not restored in hTDP-43 (+/+);mSOD1 (-/-) mice (**h**). ***$p < 0.001$.

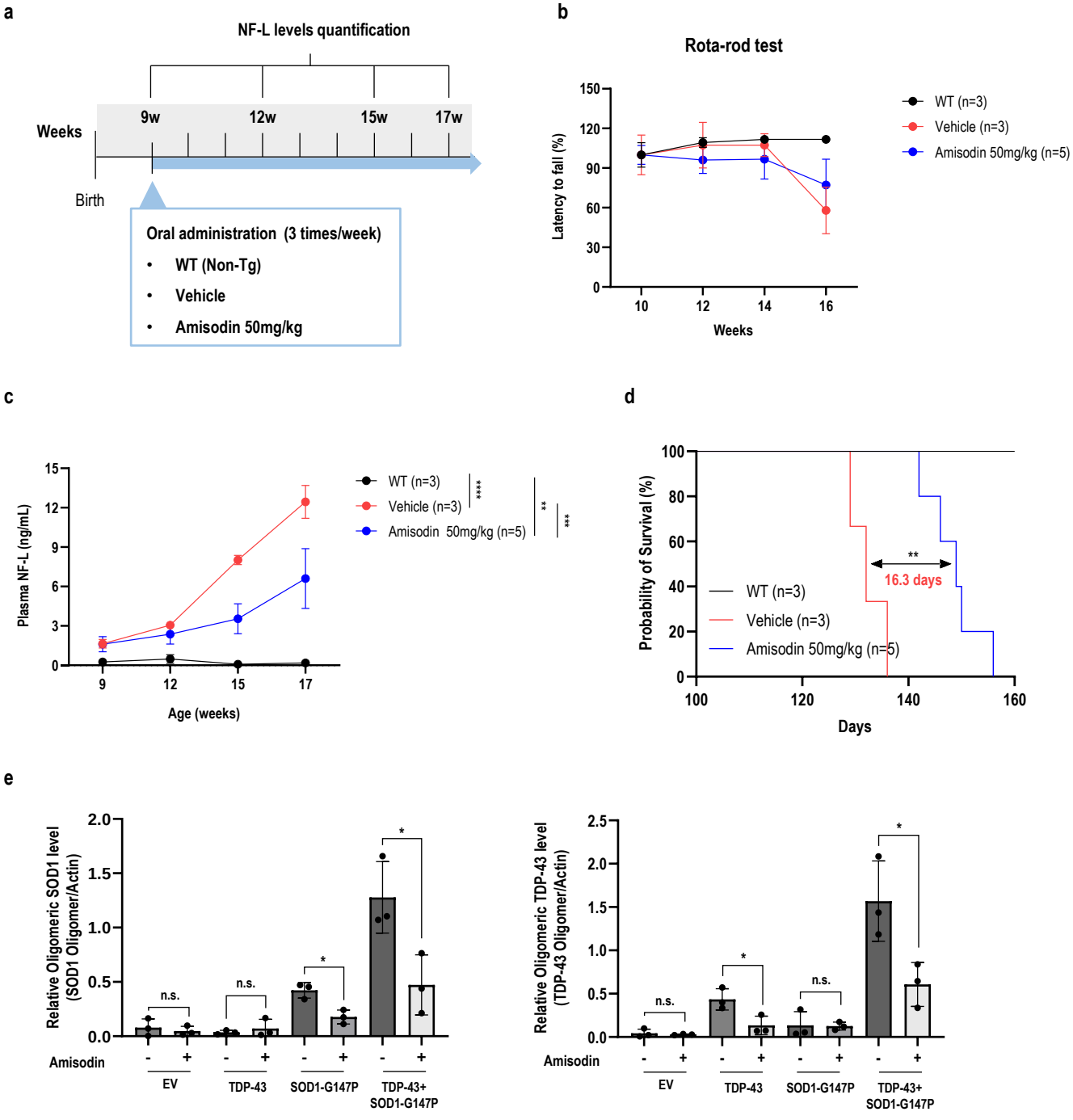

a
NF-L levels quantification
Weeks
9w
12w
15w
17w
Birth
Oral administration (3 times/week)
• WT (Non-Tg)
• Vehicle
• Amisodin 50mg/kg
b
Rota-rod test
Latency to fall (%)
Weeks
WT (n=3)
Vehicle (n=3)
Amisodin 50mg/kg (n=5)
c
Plasma NF-L (ng/mL)
Age (weeks)
WT (n=3)
Vehicle (n=3)
Amisodin 50mg/kg (n=5)
****
**
***
d
Probability of Survival (%)
Days
16.3 days
WT (n=3)
Vehicle (n=3)
Amisodin 50mg/kg (n=5)
e
Relative Oligomeric SOD1 level (SOD1 Oligomer/Actin)
Amisodin
EV
TDP-43
SOD1-G147P
TDP-43+ SOD1-G147P
n.s.
Relative Oligomeric TDP-43 level (TDP-43 Oligomer/Actin)

Fig. S7 Amisodin shows the neuro-protective effect on the SOD1$^{G93A\text{-}Tg}$ mouse model. a Schematic of Amisodin administration and assessment of neuro-protective efficacy in the SOD1$^{G93A\text{-}Tg}$ mouse model. **b** Rota-rod test exhibited improved motor performance in Amisodin-treated group compared to vehicle-treated group at 16 weeks. **c** Amisodin treatment attenuated the increase in plasma NF-L levels. $^{**}p < 0.01$, $^{***}p < 0.001$, $^{****}p < 0.0001$. **d** Amisodin-treated group exhibited an approximately 16.3 days extension in lifespan compared with the vehicle-treated group. $^{**}p < 0.01$. **e** Quantification of oligomeric TDP-43 and SOD1 levels from Fig. 5d. $^{*}p < 0.05$.

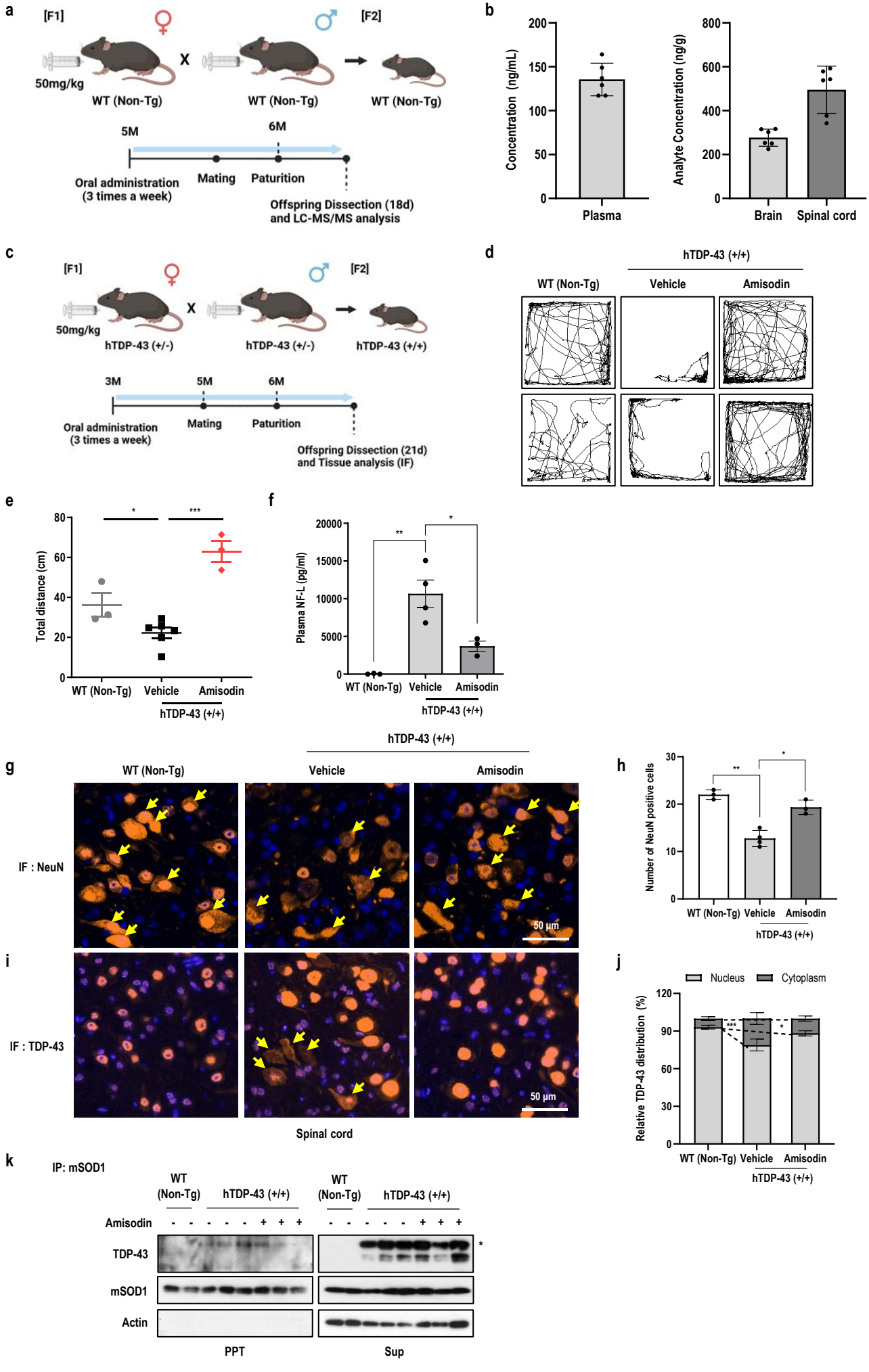
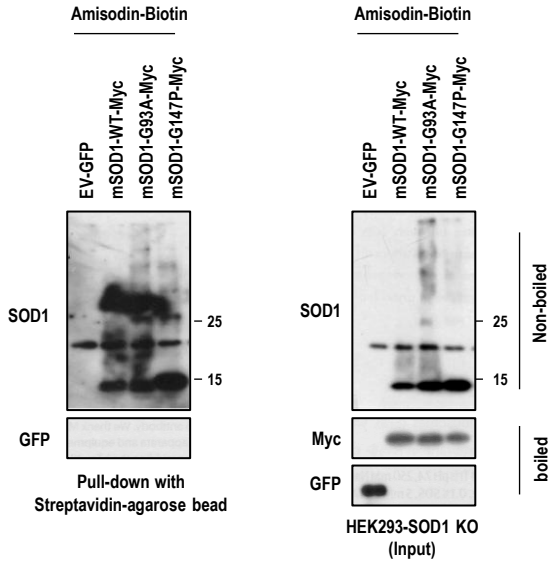
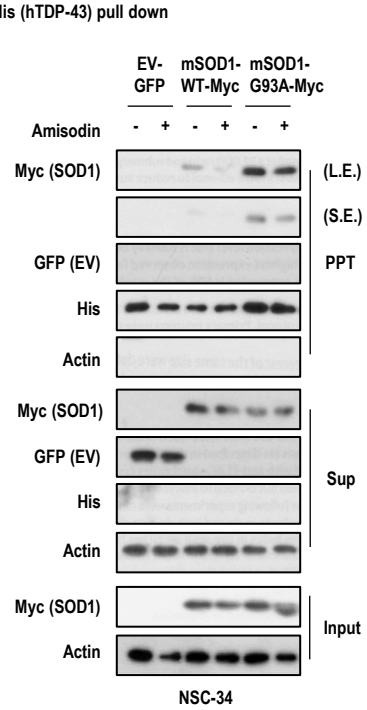

a
[F1]
[F2]
50mg/kg
WT (Non-Tg)
WT (Non-Tg)
WT (Non-Tg)
5M
6M
Oral administration
(3 times a week)
Mating
Paturition
Offspring Dissection (18d)
and LC-MS/MS analysis
b
Concentration (ng/mL)
Plasma
Analyte Concentration (ng/g)
Brain
Spinal cord
c
[F1]
[F2]
50mg/kg
hTDP-43 (+/-)
hTDP-43 (+/-)
hTDP-43 (+/+)
3M
5M
6M
Oral administration
(3 times a week)
Mating
Paturition
Offspring Dissection (21d)
and Tissue analysis (IF)
d
hTDP-43 (+/+)
WT (Non-Tg)
Vehicle
Amisodin
e
Total distance (cm)
WT (Non-Tg)
Vehicle
Amisodin
hTDP-43 (+/+)
f
Plasma NF-L (pg/ml)
WT (Non-Tg)
Vehicle
Amisodin
hTDP-43 (+/+)
g
hTDP-43 (+/+)
WT (Non-Tg)
Vehicle
Amisodin
IF : NeuN
50 μm
h
Number of NeuN positive cells
WT (Non-Tg)
Vehicle
Amisodin
hTDP-43 (+/+)
i
IF : TDP-43
50 μm
Spinal cord
j
Nucleus
Cytoplasm
Relative TDP-43 distribution (%)
WT (Non-Tg)
Vehicle
Amisodin
hTDP-43 (+/+)
k
IP: mSOD1
WT (Non-Tg)
hTDP-43 (+/+)
WT (Non-Tg)
hTDP-43 (+/+)
Amisodin
TDP-43
mSOD1
Actin
PPT
Sup

Fig. S8 Amisodin shows the therapeutic effect on the pathology in the hTDP-43 homozygous mouse model. a Schematic illustration of the experimental design for the analysis of maternal-to-offspring transfer of Amisodin. **b** Amisodin was detected in the plasma, brain and spinal cord of offspring. **c** Schematic illustration of the experimental design for the analysis of offspring from Amisodin-treated hTDP-43 (+/-) parental mice. **d, e** Representative traces of mice movement in open field test (**d**). hTDP-43 (+/+) offspring from Amisodin-treated hTDP-43 (+/-) parental mice showed increased total distance compared with offspring from vehicle-treated parents (**e**). **f** Plasma NF-L levels were significantly reduced in offspring from Amisodin-treated hTDP-43 (+/-) parental mice. **g, h** Decreased NeuN levels in hTDP-43 (+/+) mice offspring from vehicle-treated parents were significantly restored in offspring from Amisodin-treated parents. Representative confocal immunofluorescence images of NeuN in cervical spinal cord sections from mice (**g**). Scale bar, 50 μm. The number of NeuN positive cells (yellow arrows) was counted (**h**). *$p < 0.05$, **$p < 0.01$. **i, j** Increased cytoplasmic TDP-43 in hTDP-43 (+/+) mice offspring (n=3) from vehicle treated parents was significantly attenuated in offspring (n=3) from Amisodin-treated parents. WT (n=5). Representative confocal immunofluorescence images of TDP-43 in cervical spinal cord sections from mice (**i**). Scale bar, 50 μm. The relative nuclear and cytoplasmic distribution of TDP-43 was quantified by cell counting, and the percentages are presented as mean ± SD (**j**). **k** The interaction between mSOD1 and TDP-43 in spinal cord lysates was reduced in hTDP-43 (+/+) offspring from Amisodin-treated parents compared with those from vehicle-treated parents.

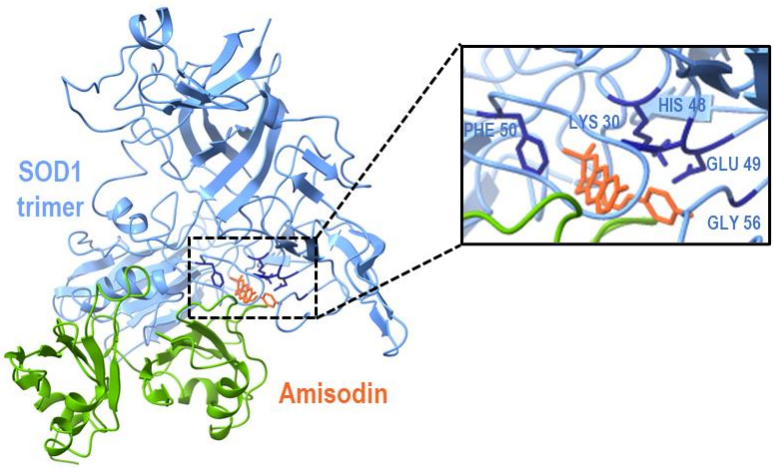
a



b



c



d Predicted molecular interaction residue of SOD1 trimer on Amisodin

Complex	Residue	Interaction type
Amisodin–SOD1 trimer	His354 (His48)	Conventional H-bond
	Gly209 (Gly56)	Conventional H-bond
	Glu355 (Glu49)	Pi–Anion
	Phe50	Pi–Sigma
	Lys336 (Lys30)	Pi–Alkyl / Carbon H-bond

e Predicted binding affinity of Amisodin and SOD1 trimer

Complex	Top Vina score
Amisodin–SOD1 trimer	-7.805 kcal/mol

Fig. S9 Amisodin reduces the SOD1-TDP-43 interaction. a Amisodin showed preferential binding to mutant mSOD1 in a streptavidin pull-down assay. **b** Amisodin disrupted the interaction between mSOD1 and hTDP-43 in NSC-34 cell lysates. Cell lysates expressing mSOD1-WT or mSOD1-G93A were incubated with Amisodin and subsequently subjected to a His pull-down assay using recombinant His-tagged TDP-43. **c-e** Predicted docking model of the SOD1 trimer–Amisodin complex and representative interacting residues are shown (**c**). A table listing the predicted interacting residues at the docking interface is presented (**d**). Predicted binding affinity of Amisodin for SOD1 trimer (**e**).

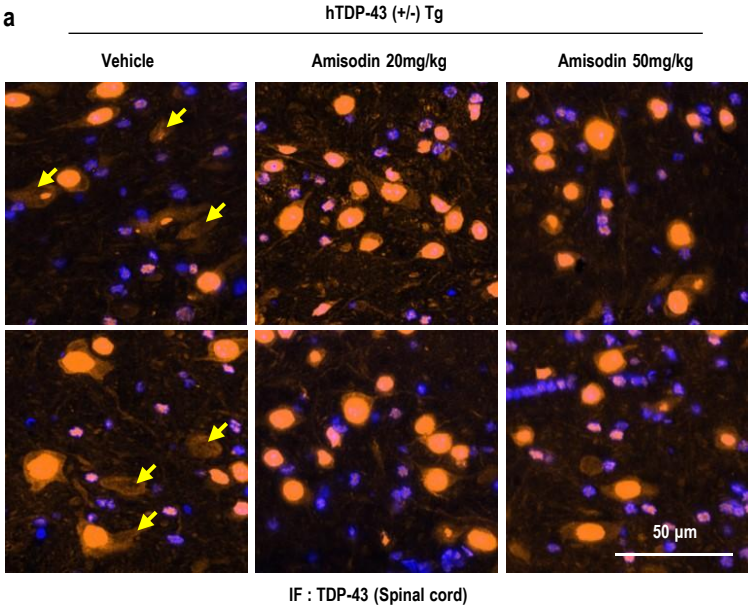

a
hTDP-43 (+/-) Tg
Vehicle
Amisodin 20mg/kg
Amisodin 50mg/kg
50 μm
IF : TDP-43 (Spinal cord)
b
Nucleus
Cytoplasm
Relative TDP-43 distribution (%)
120
90
60
30
0
**
*
Vehicle
20mg/kg
50mg/kg
hTDP-43 (+/-)
c
[Scheme of the oral efficacy study in hTDP-43 (+/-) Tg mice]
Vehicle
Amisodin 50mg/kg
hTDP-43 (+/-)
Oral administration (3 times a week)
10M
16M
Behavior tests
Dissection and
Tissue analysis (IHC)
d
WT (n=3)
Vehicle (n=3)
50 mg/kg (n=4)
hTDP-43 (+/-)
Body weight
(% of Baseline Body weight)
120
110
100
90
80
0 1 2 3 4 5 6 7 8 9 10 11 12 13 14 15 16 17 18 19 20 21 22 23 24
Weeks after Amisodin administration
e
[Vertical grid test]
Strength (N)
3.2
3.0
2.8
2.6
2.4
2.2
2.0
p = 0.0555
*
WT
(Non-Tg)
Vehicle
50mg/kg
hTDP-43 (+/-)
f
[Grip Strength test]
Time to turn (sec)
25
20
15
10
5
0
p = 0.0945
*
WT
(Non-Tg)
Vehicle
50mg/kg
hTDP-43 (+/-)
g
hTDP-43 (+/-) Tg
Vehicle
Amisodin
50 mg/kg
100 μm
IHC : NeuN (Spinal cord)
h
Number of NeuN positive cells
70
60
50
40
30
*
Vehicle
50mg/kg
hTDP-43 (+/-)

Fig. S10 Amisodin shows the therapeutic effect on the pathology in the hTDP-43 heterozygous mouse model. a, b Amisodin treatment reduced cytoplasmic TDP-43 mislocalization in the hTDP-43 (+/-) mice. Representative confocal immunofluorescence images of TDP-43 in cervical spinal cord sections are shown (**a**). Scale bar, 50 μm. The relative nuclear and cytoplasmic distribution of TDP-43 was quantified by cell counting, and the percentages are presented as mean ± SD (**b**). Vehicle (n=3), 20 mg/kg (n=6), 50 mg/kg (n=4). **c** Experimental scheme for oral Amisodin administration initiated in hTDP-43(+/-) mice at 10 months of age. **d** No significant change in body weight was observed. **e, f** Amisodin treatment improved motor impairment in hTDP-43(+/-) mice. Time to turn in the vertical grid test was reduced in Amisodin-treated mice compared with vehicle-treated hTDP-43 (+/-) mice (**e**). Grip strength was improved in Amisodin-treated mice compared with vehicle-treated hTDP-43 (+/-) mice (**f**). *$p < 0.05$. **g, h** Amisodin treatment exhibited the neuroprotective effect. NeuN immunostaining of spinal cord sections to evaluate the extent of neuronal loss and to assess the neuroprotective efficacy of Amisodin (**g**). Scale bar, 100 μm. The number of NeuN positive neurons was counted (**h**). *$p < 0.05$.